Available online at www.sciencedirect.com

jmr&t Journal of Materials Research and Technology

journal homepage: www.elsevier.com/locate/jmrt

Original Article

Effect of dispersion of alumina nanoparticles and graphene nanoplatelets on microstructural and mechanical characteristics of hybrid carbon/glass fibers reinforced polymer composite

Mohamed Abu-Okail [a], *Naser A. Alsaleh* [b], *W.M. Farouk* [c], *Ammar Elsheikh* [d,*], *Ahmed Abu-Oqail* [e], *Yasmin A. Abdelraouf* [f], *M. Abdel Ghafaar* [a]

[a] *Manufacturing Engineering and Production Technology Department, Modern Academy for Engineering and Technology, Cairo, P.O. Box 11571, Egypt*
[b] *Mechanical Engineering Department, Imam Mohammad Ibn Saud Islamic University, Saudi Arabia*
[c] *Mechanical Engineering Department, Faculty of Engineering, Benha University, Egypt*
[d] *Production Engineering and Mechanical Design Department, Faculty of Engineering, Tanta University, Tanta, 31527, Egypt*
[e] *Mechanical Production Department, Faculty of Technology and Education, Beni-Suef University, Beni-Suef, Egypt*
[f] *Chemical Engineering Department, Faculty of Engineering, Cairo University, Cairo, Egypt*

ARTICLE INFO

Article history:
Received 21 April 2021
Accepted 31 July 2021
Available online 5 August 2021

Keywords:
Hybrid carbon/glass fibers reinforced polymer
Nanocomposites
Mechanical properties
Microstructural characteristics

ABSTRACT

Dispersion of nanoparticles into fiber reinforced polymers (FRPs) has a pivotal role in strengthening their structures for critical applications such as wind turbines' blades via enhancing their mechanical properties. The current study focuses on reinforcing the FRPs used in construction of turbine blade through adding alumina nanoparticles (Al_2O_3) and graphene nanoplatelets (GNPs) to enhance the rigidity of the weak part of blades and improve their fracture toughness. Different analyses have been conducted to investigate the effect of the dispersion of nanoparticles on the microstructure of the reinforced and unreinforced samples, including optical microscope (OM), scanning electron microscope (SEM), and energy dispersive X-ray spectroscopy (EDS) and X-ray diffraction (XRD). The mechanical behavior of the reinforced and unreinforced samples was investigated in terms of tensile strength, hardness, and bending strength. Microstructural observations elucidated the achievements of excellent scattering between the matrix of FRPs and the reinforcement nanoparticles of Al_2O_3 and GNPs. The superior dispersion pattern of the nanoparticles of GNPs and Al_2O_3 inside the matrix of FRPs leads to obtain free-defects samples with extraordinary mechanical characteristics in terms of strength performance and fracture toughness.

* Corresponding author.
E-mail address: ammar_elsheikh@f-eng.tanta.edu.eg (A. Elsheikh).
https://doi.org/10.1016/j.jmrt.2021.07.158

1. Introduction

In the current era, generating clean energy from renewable resources has been considered as one of the most critical research subjects [1]. One of the recent vital sectors used in the new and renewable energy field is wind energy, in which wind turbine is used to generate energy [2]. The functionality of the wind turbine is based on the blades' criteria, composition, and manufacturing. Fiber reinforced polymers (FRPs) are the most widespread material used in manufacturing the blades of wind turbines [3]. Owing to many advantages such as mechanical characteristics and stability of thermal, electrical, and chemical properties, FRPs have been extensively used in several industries such as aerospace, automotive, and wind turbine [4–8]. Nevertheless, the usage of FRPs has some limitations due to the possible failure and damage of the weak parts of the blades caused by the exposure of different loads during the operating process [9,10]. Therefore, the properties of FRPs need to be improved by adding nanoparticles with extraordinary properties as reinforcements inside the matrix to increase the safety and durability of their usage in the wind turbine and several other applications.

Many nanoparticles such as alumina (Al_2O_3) [11–14], graphene nanoplatelets (GNPs) [15–18], and carbon nanotubes (CNTs) [18–21], as well as other nanoparticles of ceramic materials [22,23], are used as reinforcements inside the matrix of FRPs. Al_2O_3 is an entirely known nanoparticle used in several industries such as electronic insulators, substrates, and wear resistance components [24]. This is due to its high strength, stiffness, hardness, excellent resistance to wear and acid, and good thermal conductivity [25]. On the other hand, GNPs are one of the most popular nanoceramic particles, characterized by different advantages such as extraordinary mechanical and tribological properties and lower density than other nanoparticles [15].

Accordingly, the addition of Al_2O_3, GNPs, and CNTs to FRPs can improve the tensile strength, flexural strength, tribological properties, and fracture toughness [26–28]. The quality level of achievements depends on many factors such as the number of fillers, characteristics of nanoparticles (type, size, and shape, properties) and synthesis preparation, and technique type [29–31]. The combination between Al_2O_3 and GNPs as reinforcement nanoparticles inside the FRPs has a superior advantage in improving the mechanical, electrical, and thermal properties in various industries. Therefore, in the current literature, various articles have focused on the effect of nanoparticles such as Al_2O_3, GNPs, SiO_2, and CNTs on FRPs characteristics [23,32,33]. For instance, Abu Talib et al. [34] studied the effect of the addition of Al_2O_3 nanoparticles on the toughness properties of hybrid FRPs. They used different raw materials such as woven aramid fiber Kevlar-29 as reinforcement, epoxy as a matrix, and nanoparticles of Al_2O_3 as filler materials. They have been focused on three variables, namely elastic work, plastic work, and work done in the radial and tangential stretching to improve the impact characteristics of reinforced samples. They concluded that the reinforced samples were elucidated with higher energy absorption and velocity impact than unreinforced samples. A similar study was performed by Kaybal et al. [35]. They studied the influence of the addition of Al_2O_3 nanoparticles on the low-velocity impact tests of carbon fiber reinforced polymer. They used several raw materials as woven carbon fiber (CF) as reinforcement, MGS LR160 epoxy resin as matrix, while Al_2O_3 nanoparticles was used as filler materials inside the matrix. They added different weights of Al_2O_3 nanoparticles from 1 wt. % to 5 wt. % inside the resin epoxy to reinforce the strength of the matrix. They used a new route called vacuum assisted resin infusion method (VARIM) to fabricate carbon fiber reinforced polymer (CFRP) with Al_2O_3 nanoparticles without any defects such as bubbles, voids, and air spaces. They noted that the highest resistance of damage was detected at 2 wt. % Al_2O_3. Furthermore, they concluded that when adding the nanoparticles of Al_2O_3 with a weight fraction of 2% inside the resin, the energy absorption was minimized. Furthermore, Mohanty et al. [36] studied the effect of adding Al_2O_3 nanoparticles on the impact and flexural characteristics of hybrid short glass and carbon fibers. They used some raw materials such as chopped glass and carbon fibers with a length of 1–7 mm as reinforcement; epoxy Bondtite PL-411 as the matrix, and Al_2O_3 as nanofiller material. They used different weights percentage of Al_2O_3 from 1 wt.% to 5 wt.% inside the matrix. They used the open casting technique by a mechanical stirrer to produce the samples with a homogenous dispersion of Al_2O_3 nanoparticles inside the matrix. They elaborated that the nanoscale of Al_2O_3 with 2% achieved the optimum impact and flexural characteristics (strength and modulus) and thermal stability. On the other hand, when the amount of Al_2O_3 nanoparticles increased to 5 wt.%, the dispersion of Al_2O_3 nanoparticles was aggregated, causing poor characteristics of the fabricated samples.

Another study was carried out by Li et al. [37]. They studied the influence of the addition a hybrid CNTs + Al_2O_3 on the mechanical characteristics such as flexural modulus and shear strength as well as microstructural properties as interfacial interactions of glass fiber reinforced polymer (GFRP). They used different raw materials such as woven GF as reinforcement, epoxy resin as matrix, and a hybrid of CNTs + Al_2O_3 as filler nanoparticles inside the resin. They mixed these materials by the chemical vapor deposition method. They observed that the dispersion of hybrid of CNTs + Al_2O_3 was homogenous inside the whole matrix, assisting on the hindrance of the crack occurrence. They concluded that the reinforced samples with a hybrid of CNTs + Al_2O_3 showed the highest flexural modulus and shear strength properties. Moreover, Mudra et al. [38] synthesized and characterized fiber-reinforced ceramic composites. They selected some materials as monolithic Al_2O_3 as reference material and Al_2O_3 as the matrix. They synthesized two cases; the first case is GNPs coated Al_2O_3 fibers, while the second case is GNPs coated Al_2O_3 powders. The first and second cases were at the micro and nanoscale. They used different combination techniques such as electro-spinning, calcination, chemical-vapor-deposition (CVD), and spark-plasma-sintering (SPS) to prepare these compositions. They noted that the addition of GNPs assists in improving the lubrication characteristics, fracture toughness, and electrical conductivity of ceramic

nanocomposites. They also interpreted that the GNPs coated Al_2O_3 fibers and GNPs coated Al_2O_3 powders were presented the highest hardness, fracture toughness, and electrical conductivity. This is due to the better dispersion of GNPs coated polycrystalline Al_2O_3 fibers inside the matrix of Al_2O_3.

Generally, in the wind energy industry, there are several manufacturing techniques for fabricating the blade. According to literature, the most commonly used techniques are: hand lay-up, prepreg technology, resin transfer molding (RTM) and vacuum infusion (VI).

Hand lay-up and compression-molding techniques were selected in the current study due to their availability and reasonable costs under Egyptian conditions.

Based on the previous studies, the experimental work carried out on the addition of more than one sturdy reinforcement nanoceramic particle into the matrix of FRPs is limited. Furthermore, the syncretization, characterizations, and optimizations of the filler amount in more than one sturdy reinforcement powders to the matrix of FRPs are rarely studied. Therefore, the main aim of the current contribution is to synthesize, characterize and optimize the addition of more than one sturdy reinforcement nanoceramic particles such as Al_2O_3 and GNPs to the matrix of hybrid FRPs. Accordingly, the specific objective of this study is to investigate the effect of adding nanoparticles of Al_2O_3 and GNPs and their dispersion on hybrid carbon and GFRP in terms of microstructural and mechanical properties for wind turbine applications. The experimental work, followed by the results and discussion, will be briefly discussed in Sections 2 and 3. To end up with the conclusion that will be summarized in Section 4.

2. Materials and experiments

This section briefly explains the experimental work procedures, including the material chosen, its specifications, the technique, and the tools used.

In this work, two kinds of fibers, including E-glass fiber with a density of 2.56 g/cm^3 and carbon fibers with a density of 1.6 g/cm^3, were used to produce different composite structures. Carbon fiber and glass fiber were supplied from Arab World for Financial Investments Company, Cairo, Egypt. Each type of fabric consisted of two sets of perpendicularly interlaced fiber yarns, the warp or longitudinal direction, and the fill or transverse direction, as shown in Fig. 1 (a,b). Sikadur resin (Sikadur 330) is an epoxy supplied by Sika Corporation used as a matrix between the different kinds of used fibers, which is also suitable for vacuum infusion. On the other hand, two types of nanoparticles: aluminum oxide (Al_2O_3) and graphene nanoplatelets (GNPs), were used as nano reinforcements inside the resin matrix. GNPs and Al_2O_3 were supplied from Nano Gate Company for nanomaterials and Chemicals, Cairo, Egypt. The nanopowders of Al_2O_3 were a white color, spherical-like shape, $\leq$25 nm, density 3.78 g/cm^3, purity~ 95%, tensile strength 665 MPa, as shown in Fig. 1(c). On the other hand, the nanopowders of GNPs were gray in color and fine flake in shape with an average size of 100 nm, as shown in Fig. 1(d). The physical and mechanical properties of epoxy resin, E-glass fiber, carbon fiber, Al_2O_3, and GNPs are listed in Table 1. Fiber volume fraction (v_f) was measured experimentally by removing the matrix of epoxy by burning and chemical techniques according to ASTM D-3171-99 [19].

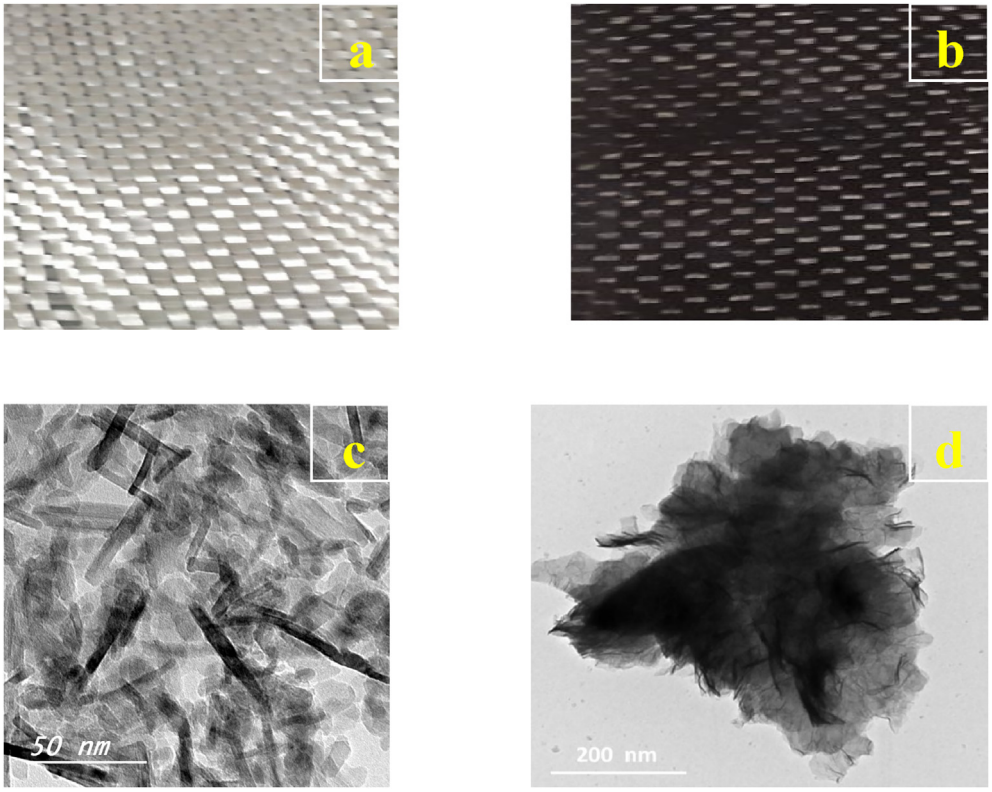

Fig. 1 – (a) woven glass fiber, (b) woven carbon fiber, (c) Al_2O_3, and (d) GNPs.

Table 1 – Physical and mechanical properties of epoxy resin, E-glass fiber, carbon fiber and Al_2O_3 as well as GNPs.

Properties	Epoxy	E-glass fiber	Carbon fiber	Al_2O_3	GNPs
Density (g/cm^3)	1.16	2.56	1.6	3.78	2.267
Tensile strength (MPa)	30	1400	2400	665	167
Tensile modulus (GPa)	4.1	72.3	228	210	2.4 * 10^3
Poisson's ratio	0.35	0.22	0.30	0.24	0.012

The average volume fraction was kept at 64%. The specifications of the constituents proposed for the current work are listed in Table 2. Different types of composite structures were selected and carried out, as shown in Table 2. It can be noted that the hybrid structure consists of a combination between two woven layers of glass fiber and two woven layers of carbon fiber mixed with the polymer resin.

The nanoparticles of Al_2O_3 and GNPs were mixed inside the epoxy resin matrix using the ultrasonication process shown in Fig. 2. The mixing process was executed at mixing time of 30 min at 500 RPM by Henan Lanphan mechanical stirrer to obtain uniform and homogenous dispersion. Hielscher ultrasonic processor UP200S with 200 W and frequency 24 kHz performed the sonication process. Beni-Suef University supplied the ultrasonic processor. The sonication process was performed at 0.5 cycles per second with 70% amplitude for 3 h. To prevent the agglomeration of nanoparticles, the sonication time should be long enough. An important point must be mentioned. To prevent resin degradation, it must be long waiting until cooling the epoxy mixture and nanoparticles by putting on an ice water bath before preparing sonication. Then the hardener and epoxy resin were mixed with recommended ratio. The ratio of hardener to epoxy was kept 1:2 by weight. The curing cycle of all produced samples was at 55 °C for 30 min.

Graphene is used as a reinforcement nanomaterial due to its superior characteristics such as higher young modulus (>1 TPa), lower density (1.06 g/cm3) and higher fracture strength (130 GPa). Furthermore, graphene nano-platelets possess thrilling attributes such as lightweight, wide aspect ratio, electric and thermal conductance, mechanical strength, and reasonable cost. These characteristics make the graphene one of the most important nano-reinforcement materials nano-composite field, especially in the modern industrial applications [39]. Moreover, the addition of GNPs composite material helps to improve the dimensional stability and operating temperature tolerance. On the other hand, Al_2O_3 has enhanced optoelectronic and physiochemical properties. There are numerous applications of GNPs and Al_2O_3 nanoparticles that it would be too long for this brief introduction. The advantages of these nanoparticles are immense but they are not without their drawbacks. So, The combination of graphene and alumina (GNPs– Al_2O_3 nanocomposites) inside the matrix of hybrid glass and carbon fibers reinforced polymer matrix composites has a significant benefit towards its mechanical, electrical, and thermal properties. On the other hand, Al_2O_3 powders have fine spherical particle shape with particle size 50 nm, while, the GNPs powders have a fine flake shape with an average size of 100 nm. Specifically, graphene nanoplatelets are unique nanoparticles consisting of short stacks of graphene sheets having a platelet shape. So, the adding different shapes as Al_2O_3 (fine spherical particle shape) and GNPs (fine platelet shape) inside hybrid glass and carbon fibers reinforced polymer matrix composites are assisting to merge the matrix materials and reinforcement constituents, which is refilling any bubbles, voids and porosities inside the microstructure.

To fabricate different types of composite structures, two manufacturing methods were used hand lay-up and compression-molding techniques. In the technique of hand lay-up, the layers of woven fabrics were placed on a flat and smooth surface with an insulator in between plastic sheets as a release agent. Nanoparticles were prepared by surface treatment of nanoparticles using stearic acid as a non-reactive modifier. This is to increase the adhesion between the nanoparticles and the epoxy. However, stearic acid was added to ethyl-acetate solution with stirring for ½ hour by an electric mixer at a speed of 900 rpm. Then the nanoparticles are added to the mixture with stirring for another ½ hour, followed by the process of washing the nanoparticles using ethyl-acetate solution and filtrate until the excess stearic acid is removed. It was followed by carefully adding epoxy with nanoparticles with intermittent stirring for 30 min at 500 rpm. Next, add the mixture to the first layer of woven fabrics. While making sure that the first layer of woven fabrics is saturated with epoxy, the second layer of woven fabrics is added sequentially. Then the process continued until the completion of the number of layers required. On the other hand, the compression mold technique was used through preparing the mold with a flat and good

Table 2 – Different kinds of composite structures used in present experimental procedures.

No.	ID specimens	Name specimens	Reinforcement type	Matrix type	Nano kind and weight percentage
1	S_1	Glass fibers	Glass fibers	Sikadur 330 epoxy	Without
2	S_2	Carbon fibers	Carbon fibers		Without
3	S_3	Hybrid glass and carbon fibers	Carbon fibers + Glass fibers		Without
4	S_4	Hybrid glass and carbon fibers at1.5% wt. GNPs+ 1.5 % wt. Al_2O_3	Carbon fibers + Glass fibers		1.5% wt. GNPs+ 1.5 % wt. Al_2O_3
5	S_5	Hybrid glass and carbon fibers at 3% wt. Al_2O_3	Carbon fibers + Glass fibers		3%wt. Al_2O_3

surface finishing, and internal dimensions 300 × 200 mm were covered with a transparent plastic sheet as a release agent, as shown in Fig. 2. After curing, samples are machined according to the standard specifications for each test.

After the manufacturing stage, samples were examined by microstructural and mechanical tests. Optical microscope (OM), scanning electron microscope (SEM), and energy dispersive X-ray spectroscopy (EDS), and X-Ray diffraction (XRD) were used to evaluate the macro and microstructural characterization of the reinforced and unreinforced samples. Hardness test was carried out by Shimadzu Vickers microhardness testing device for the reinforced and unreinforced samples at 200 g load and 10 s. Tensile tests were carried out on a universal testing machine at room temperature following the ASTM standard recommendations. The bending test was performed by the universal testing machine using three points method at standard temperature. The diameter of the rollers was 30 mm while the distance between the rollers was 37 mm. The speed of the crosshead during the bending test was kept at 2 mm/min for all tests. After presenting the details of experimental work, we can be introduced the results and discussions.

3. Results and discussion

3.1. *Microstructural characteristics of produced hybrid FRPs with additional nanoparticles*

This section illustrates the influence of nanoparticle addition on the microstructural characteristics of hybrid FRPs through the observations of the OM, SEM, EDS and XRD.

Fig. 3 shows the optical microscope of the prepared samples at different conditions. As we can see in the first case of glass fibers in (a), different bubbles can be noted at the prepared surface's macroscale. This is due to different items such

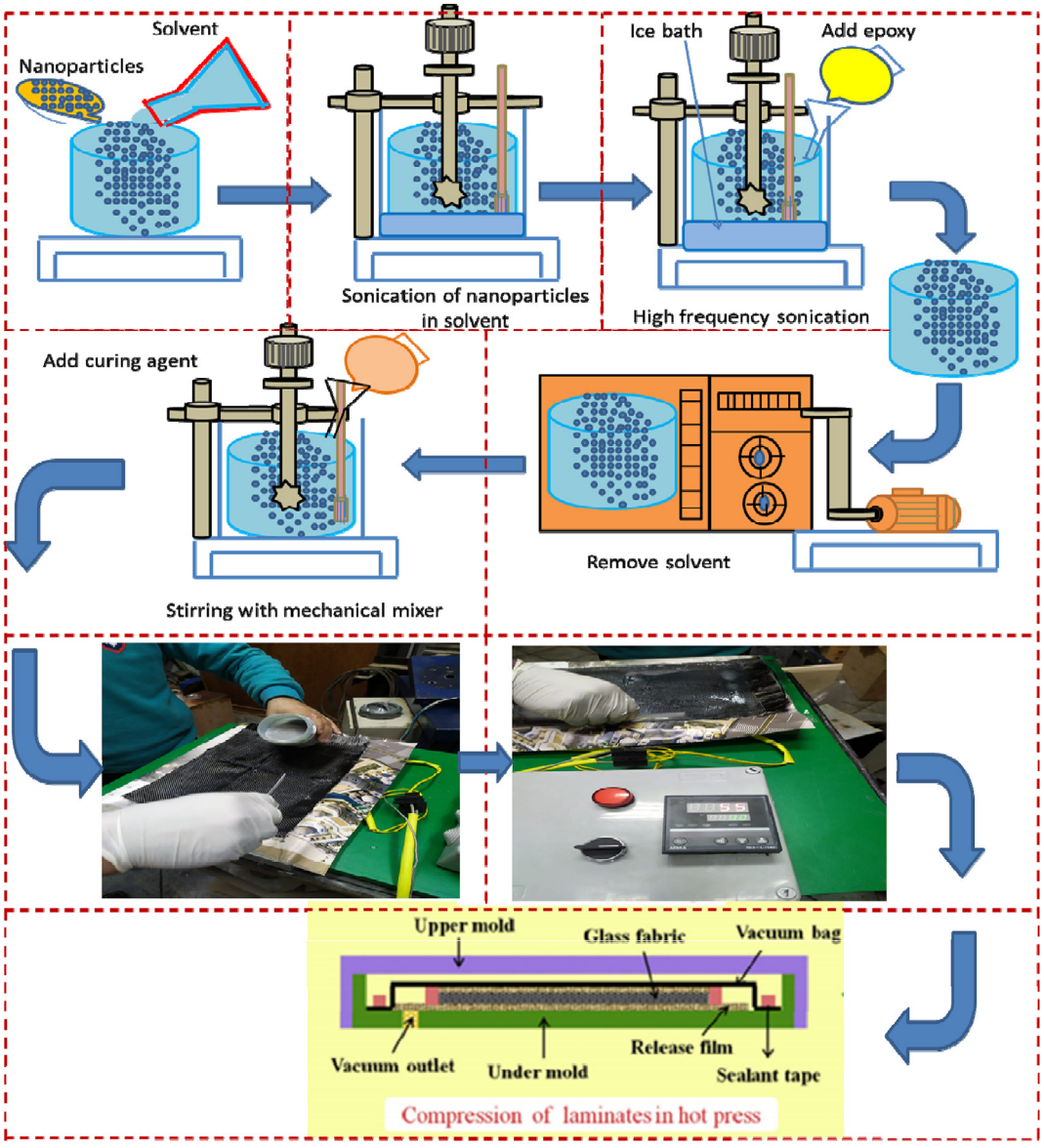

Fig. 2 – Schematic and actual fabrication sequences of prepared hybrid carbon and glass fibers with and without adding nano particles of Al_2O_3 and GNPs.

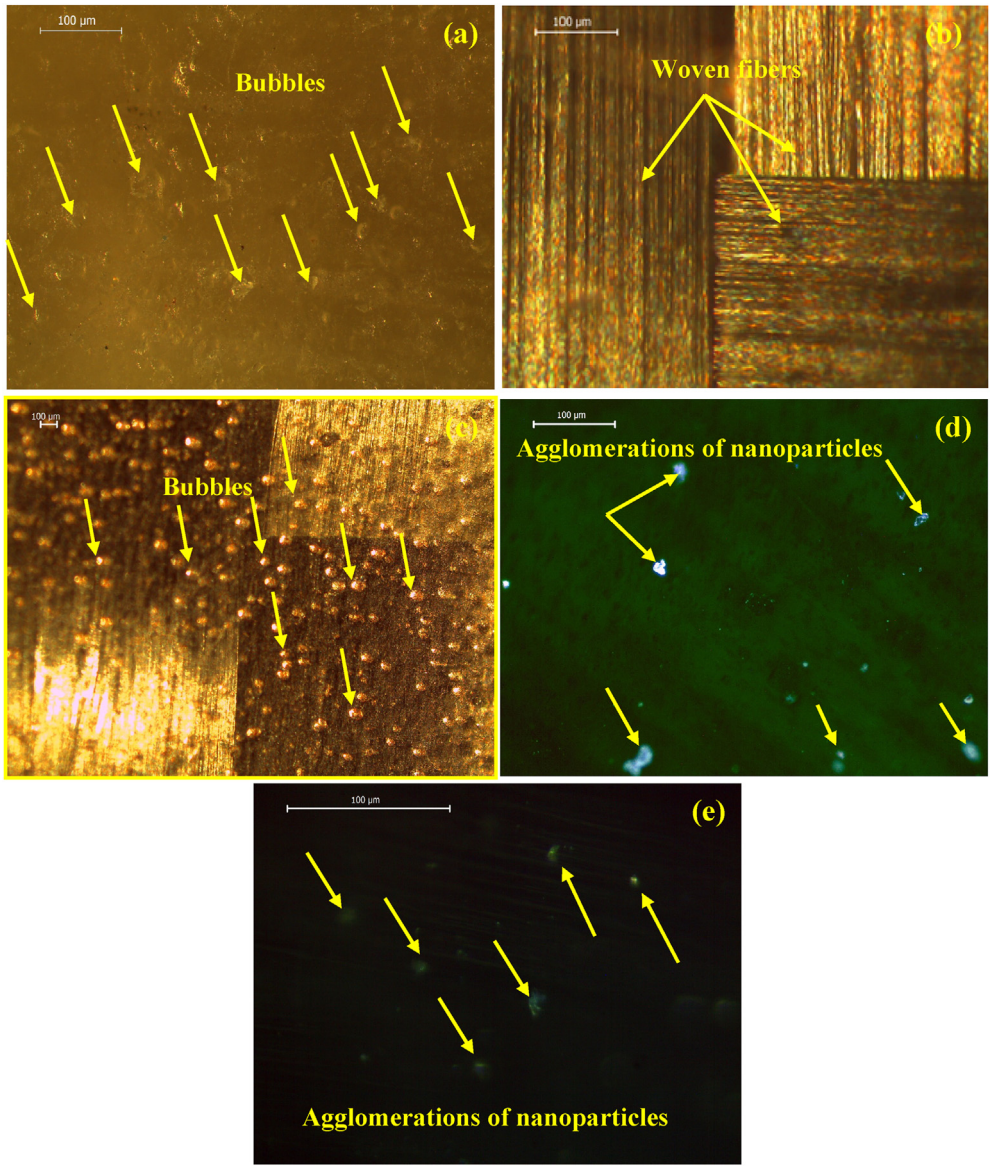

Fig. 3 – Optical Microscope of prepared samples at: (a) S_1, (b) S_2, (c) S_3, (d) S_4 and (e) S_5.

as (i) the distance between woven glass fibers is large, (ii) the high amount of resin compared to the fibers contents, and (iii) the insufficient compression pressure of laminate at the hot press. All these elements are caused by the appearance of the bubbles and voids between these fibers. In the second case of carbon fiber in (b), it can be observed that the woven carbon fibers have appeared without any bubbles in the macroscale, this is due to the distance between woven fibers is suitable, and the interaction between the resin and carbon fibers is sufficient. On the other hand, the third case of hybrid glass and carbon fibers without nanoparticles in (c) illustrated different bubbles and voids between the hybrid glass and carbon fibers. This is due to the differences between dimensions, interactions, and volume fractions of the glass and carbon fibers. Based on the above observations, it is essential to add the nanoparticles embedded inside these bubbles and voids to fill the gaps between hybrid glass and carbon fibers. In the fourth case of hybrid glass and carbon fibers with nanoparticles at weight fraction of 1.5% of GNPs and weight fraction of 1.5% of Al_2O_3 in (d), it can be observed that some nanoparticles of GNPs and Al_2O_3 are scattered between hybrid glass and carbon fibers, which fill the gaps and eliminate the appearance of any bubbles and voids inside the prepared sample. Finally, in the fifth case, hybrid glass and carbon fibers with nanoparticles at weight fraction of 3% of Al_2O_3 in (e), it can be observed that the agglomerations of Al_2O_3 nanoparticles were formed between the hybrid glass and carbon fibers, which help in preventing the occurrence of any voids and bubbles.

Fig. 4 reveals the scanning electron microscope of the prepared samples at different conditions. In the sample of glass fiber, it can be observed that the nanopores exist between the glass fibers. While in the carbon fiber sample, the nanovoids are indicated but lower than in the sample of glass

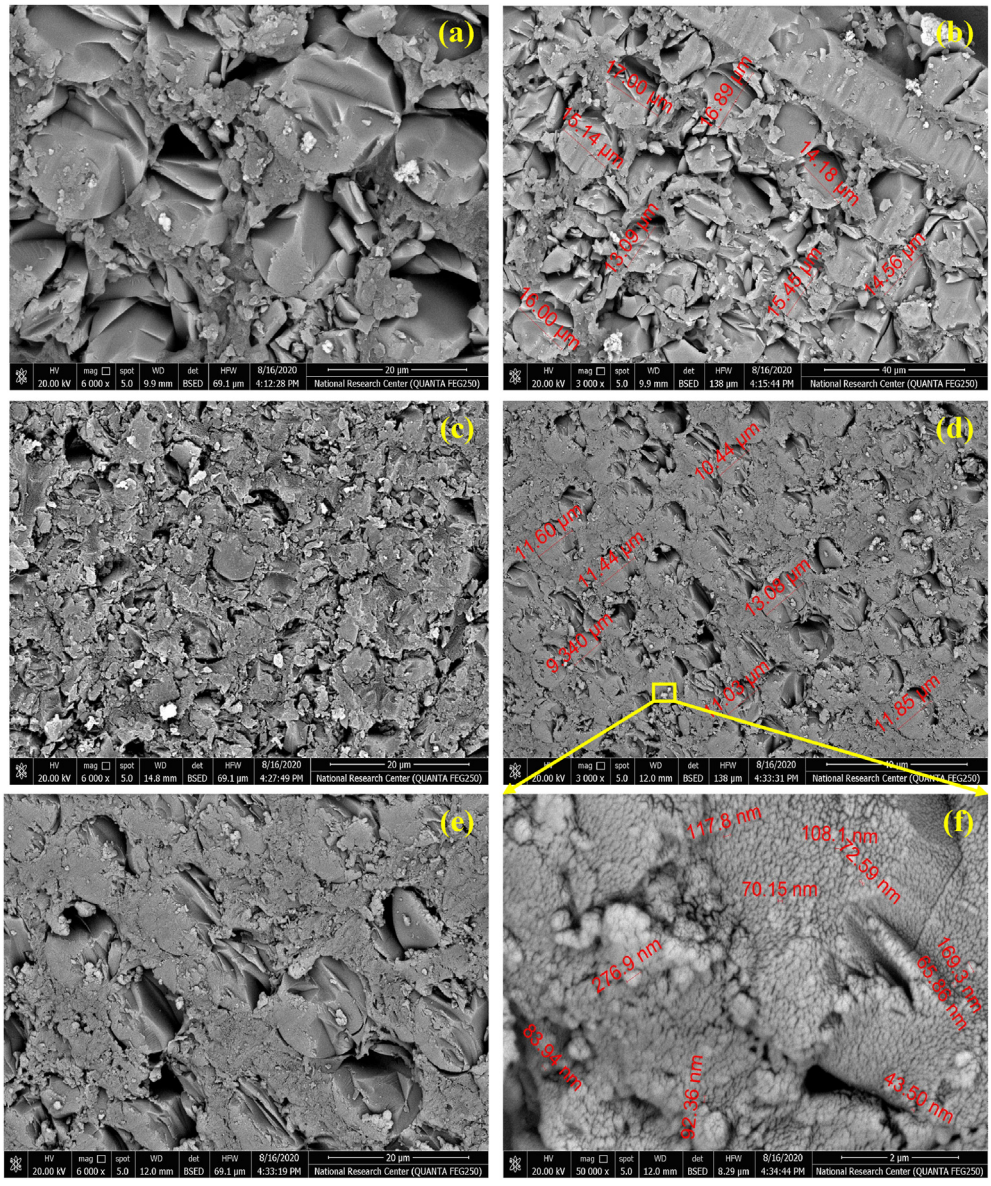

Fig. 4 – Scanning Electron Microscope of prepared samples at: (a) S_1, (b) S_2, (c) S_3, (d) S_4, (e) S_5 and (f) high magnification scale at S_4.

fibers. On the other hand, nanobubbles are observed in the sample of hybrid glass and carbon fibers without nanoparticles. This is due to the differences between density, dimension, and distance between woven fibers. However, uniform scattering of nanoparticles was observed in the samples of hybrid glass and carbon fibers at weight fraction of fraction of 1.5% for both of GNPs and Al_2O_3. This endued to different benefits such as: (i) reduce the concentration ratio, which assisted in preventing the agglomeration, (ii) improve the strengthening mechanism of the resin matrix, (iii) increase the inter-laminar adhesion between the matrix and fiber through incorporating mixed nanoparticles of Al_2O_3 and GNPs, (iv) convert the stress concentration from matrix to the fiber as well as, and (v) enhance the mechanical properties of the prepared samples. Furthermore, the thin layer of GNPs cannot act as a reinforcing element. Still, the mixed compositions between Al_2O_3 and GNPs were assisted in reinforcing the process through the adhesion of the GNPs with the carbon fiber and glass fiber, and then Al_2O_3 nanoparticles are bonded by them via the connections of GNPs with the carbon fiber and glass fiber. On the other hand, in the sample of hybrid glass and carbon fibers at weight fraction of 3% of Al_2O_3, agglomerations of Al_2O_3 nanoparticles is observed that weakened the bonding between the matrix and fiber. This is due to the unbalance of the corporation of nanoparticles in this sample. Fig. 5 presents the field emission scanning electron microscopes (FE-SEM) image and mapped analysis of C, O, and Al for a prepared sample at hybrid glass and carbon fibers at weight fraction of 1.5% of GNPs and weight fraction of 1.5% of Al_2O_3. The FE-SEM observation of the prepared sample at hybrid glass and carbon fibers at weight fraction of 1.5% of GNPs and weight fraction of 1.5% of Al_2O_3 was showed

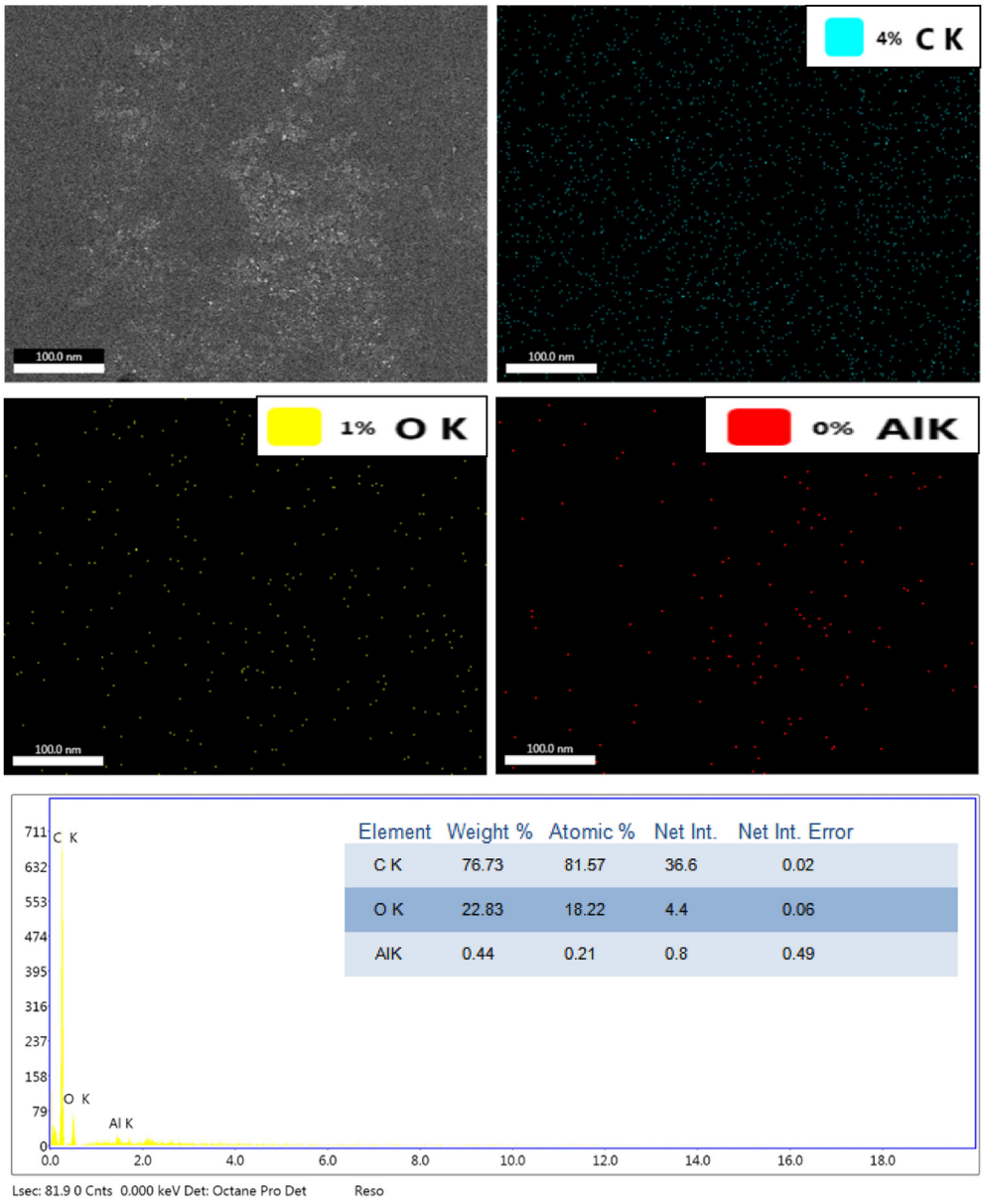

Fig. 5 – FE-SEM image and map analysis of C, O and Al for prepared sample at hybrid glass and carbon fibers at weight fraction of 1.5% of GNPs and weight fraction of 1.5% of Al_2O_3.

homogenously scattering of mixed nanoparticles of Al_2O_3 and GNPs in the whole surface. This is due to the efficient sonication process. According to map analysis, it can be noted that the elements of C, O, and Al are embedded between the matrix and fiber. The EDS analysis of the mixed nanoparticles at weight fraction of 1.5% of GNPs and weight fraction of 1.5% of Al_2O_3 are showed the intensity of C, O, and Al elements. It can be illustrated that the C intensity is the highest while the Al is the lowest. The C is expressed as the GNPs and carbon fiber, and glass fiber as well as Al is expressed as the Al_2O_3. On the other hand, the element of O is expressed as the nanobubbles.

Fig. 6 shows XRD patterns of the prepared samples. Generally, it can be elucidated that the intensity of the element of C and Al_2O_3 were showed a reduction in all peaks. This is due to the similarity and addition of nanoparticles as GNPs and Al_2O_3 with carbon fiber and glass fiber in the prepared samples. Specifically, the intensity of the C element in all conditions was observed as the highest intensity. This is also due to the resemblance of additive nanoparticles as GNPs and glass and carbon fiber.

On the other hand, the element intensity of Al_2O_3 exhibited the lowest. The XRD spectra of S_1, S_2, and S_3, as well as S_4 and S_5 show the element of C in 18, 25 and 38, and 42 and 44°, respectively, of 2Θ at x-axes. This proved the appearance of glass and carbon fiber in all prepared samples, and also that was proven the appearance of GNPs in the S_4. On the other hand, in S_4 and S_5, the element of Al_2O_3 was observed at 23 and 43 degrees of 2Θ at x-axes. This proved the appearance of Al_2O_3 in the hybrid glass and carbon fiber with different additions in S_4 and S_5, which helps in improving the mechanical

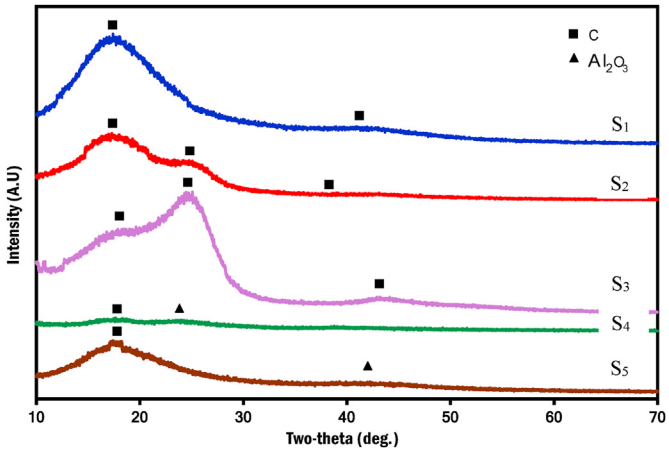

Fig. 6 – XRD patterns of prepared samples at: (a) S_1, (b) S_2, (c) S_3, (d) S_4 and (e) S_5.

properties. Investigation of the mechanical characterizations will be explained briefly in Section 3.2.

3.2. *Mechanical properties of produced hybrid FRPs with nanoparticles*

This section illustrates the effect of nanoceramic particles on the mechanical properties of hybrid FRPs by hardness, tensile and bending tests.

Fig. 7 shows the Vickers microhardness maps of the cross-section of prepared samples at different conditions. Generally, the microhardness maps explain the hardness distribution based on adding nanoparticles in two axes, x, and y, in all prepared samples. According to Fig. 7, it can be noted that the lowest hardness was observed at hybrid glass and carbon fibers without nanoparticles in (c). This is because the nanoparticles are not added, which is caused by nanobubbles in this sample. On the other hand, the highest hardness was shown at hybrid glass and carbon fibers at weight fraction of 1.5% of GNPs and weight fraction of 1.5% of Al_2O_3 in (d). This is due to the sufficient dense concentration of nanoparticles and uniform scattering of nanoparticles. Specifically, in the glass fiber sample, the hardness map shows different values begin from minimum value 4 VHN until maximum value 8 VHN scattering in the whole of the cross-section of the prepared sample. Furthermore, in the carbon fiber sample, the hardness map illustrates different values beginning from a minimum value of 7 VHN until a maximum of 12 VHN. Moreover, in the sample of hybrid glass and carbon fibers without nanoparticles, the hardness map elucidates different values from a minimum value of 0.6 VHN to a maximum of 1.8 VHN. On the other hand, in the sample of hybrid glass and carbon fibers at weight fraction of 1.5% of GNPs and weight fraction of 1.5% of Al_2O_3, the hardness map observes different values begin from minimum value 9 VHN until maximum value 14 VHN. Finally, in the sample of hybrid glass and carbon fibers at weight fraction of 3% of Al_2O_3, the hardness map shows different values begin from minimum value 0.5 VHN until maximum value 3 VHN. According to the hardness measurements, it can be proven that the sample of hybrid glass and carbon fibers at weight fraction of 1.5% of GNPs and weight fraction of 1.5% of Al_2O_3 was optimum. This is due to better distribution and an excellent scatter and dense of nanoparticles inside the matrix.

Fig. 8 shows the tensile strength of prepared samples at different conditions. According to Fig. 8, it can be elucidated that the first sample (S_1) showed ultimate tensile strength and elongation at 52 MPa and 0.048, respectively. However, the behavior of the S_1 sample was brittle. The second sample (S_2) showed ultimate tensile strength and elongation at 142 MPa and 0.042, respectively. An important point that can be mentioned here is the ultimate tensile strength and elongation of both glass fiber and carbon fiber samples in S_1 and S_2 were seem uncharacteristically low. This is due to the bubbles that formed on the surface of the prepared samples in macro and nano-scale. While, the third sample (S_3) was observed ultimate tensile strength and elongation at 133 MPa and 0.073, respectively. On the other hand, the fourth sample (S_4) showed ultimate tensile strength and elongation at 162 MPa and 0.049, respectively. Moreover, the fifth sample (S_5) showed ultimate tensile strength and elongation at 230 MPa and 0.057, respectively. It can be noted that the additive of nanoparticles improved the strength from 52 MPa at glass fiber without nanoparticles to 230 MPa at the hybrid glass and carbon fiber with weight fraction of 3% of Al_2O_3. Moreover, it can also be noted that the additive nanoparticles improved the strength from 133 MPa at the hybrid glass and carbon fiber without nanoparticles to 230 MPa at the hybrid glass and carbon fiber with weight fraction of 3% of Al_2O_3. This is due to better uniform scattering of nanoparticles and sufficient dense concentration of nanoparticles. This is assisted in improving the mechanical properties of wind turbine structures. Due to the direct relation between bending and other mechanical properties such as strength and ductility, further discussions about them will be explored in the next section.

The effect of adding nanoceramic particles on the mechanical properties of hybrid FRPs by the bending test was investigated. The bending test was carried out based on three-points flexural tests at room temperature to deeply understand how far the composite could resist against the flexural loading over different ranges of particles and fiber loading in

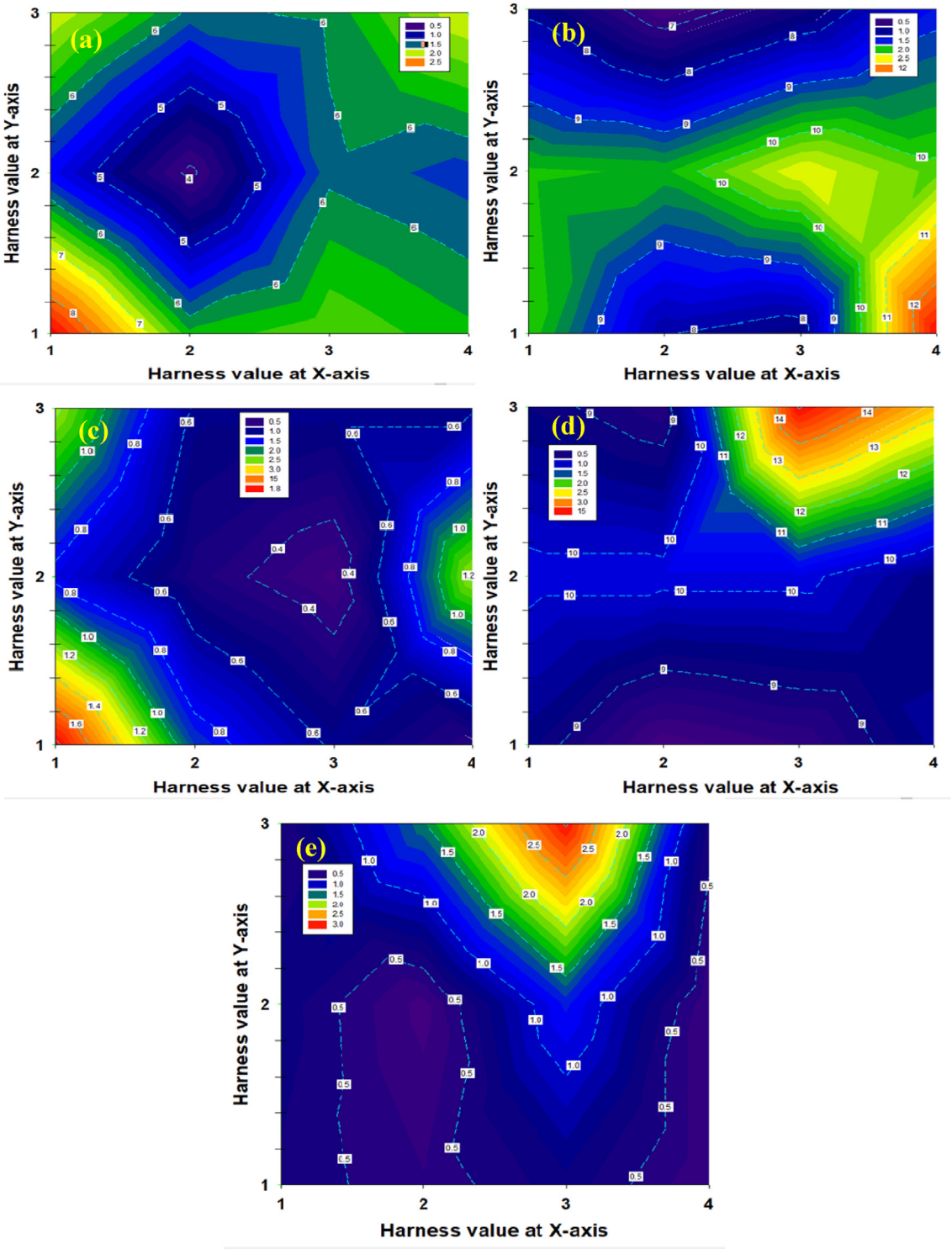

Fig. 7 – Hardness measurements of prepared samples at: (a) S_1, (b) S_2, (c) S_3, (d) S_4, and (e) S_5 at x and y-axes.

the epoxy matrix. Fig. 9 shows the effect of nanoparticles on the flexural strength of hybrid carbon and glass fiber. As shown in Fig. 9, the highest flexural load was obtained in the hybrid glass and carbon fiber at weight fraction of 3% of GNPs. While, the lowest flexural load was observed in hybrid glass and carbon fiber at weight fraction of 1.5% of GNPs and weight fraction of 1.5% of Al_2O_3. On the other hand, the glass and carbon fiber and hybrid glass and carbon fiber were obtained medium flexural load. The highest weight composition of GNPs nanoparticles in the epoxy matrix (weight 3%), the highest concentration of the flexural strength, decreases after that in weight fraction of 1.5% of GNPs and weight fraction of 1.5% of Al_2O_3 nanoparticles in the epoxy matrix. Specifically, it was observed that the flexural strength of specimens with

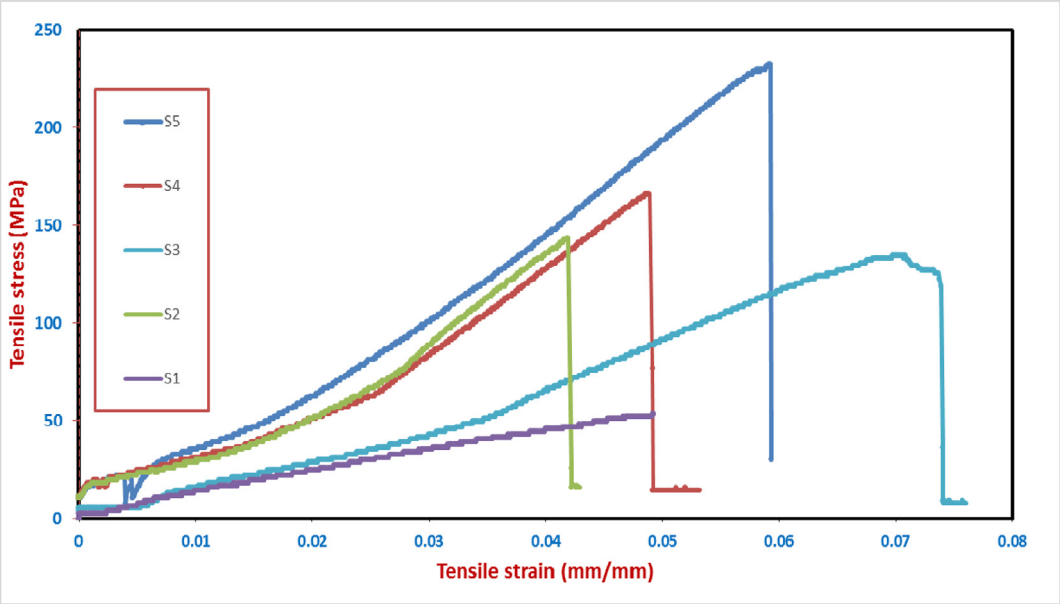

Fig. 8 – Tensile strength of prepared samples at: (a) S_1, (b) S_2, (c) S_3, (d) S_4, and (e) S_5.

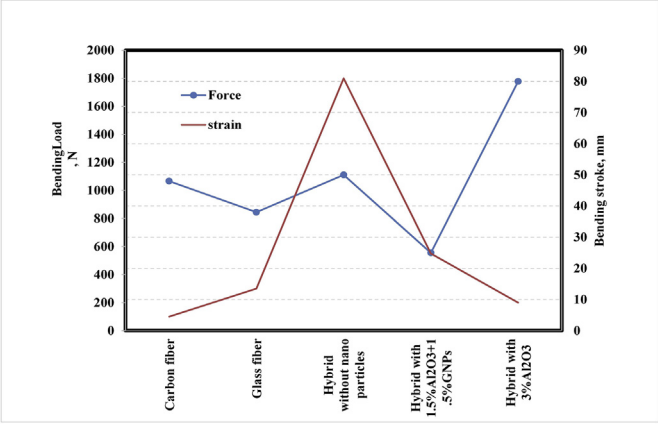

Fig. 9 – Bending strength of prepared samples at: (a) S_1, (b) S_2, (c) S_3, (d) S_4, and (e) S_5.

Al_2O_3 nanoparticles attained their optimum value at a weight fraction of 3% and gradually decreased after the high concentration of weight fraction of 1.5% of GNPs and weight fraction of 1.5% of Al_2O_3. The highest concentration of flexural strength was due to the nanoparticle's enhanced dispersion in the epoxy matrix. At the same time, the aggregation of nanoparticles reduces the concentration of flexural strength of the nanocomposites. The flexural modulus of hybrid glass and carbon fiber nanocomposites also increases with the addition of Al_2O_3 and GNPs nanoparticles.

On the other hand, the flexural strain of carbon fiber was at its lowest value, while the flexural strain of hybrid glass and carbon fiber without nanoparticles was the highest. This is due to the appearance of the bubbles and voids, which are increasing the distance between the grain boundaries that assisted in absorbing any deformations. While, the flexural strain of glass fiber, hybrid glass, and carbon fiber at weight fraction of 1.5% of GNPs and weight fraction of 1.5% of Al_2O_3 and hybrid glass and carbon fiber at weight fraction of 3% of Al_2O_3 were medium.

Fig. 10 shows the fracture surfaces of prepared samples at different conditions under tension test. However, according to Fig. 10, it can be elucidated that the tension failure of fibers was observed at the first case of glass fiber in (a). This is due to the appearance of voids and bubbles. On the other hand, the pull out cavity was elucidated at the second case of the carbon fiber in (b). In the third case of hybrid glass and carbon fibers without nanoparticles the brittle fracture was observed in (c). This is due to the nanoparticles are not added. The mixed modes of failure as tension failure of fibers and pull out cavity were observed at hybrid glass and carbon fibers with nanoparticles at 1.5 wt. % Al_2O_3 and 1.5 wt. % GNPs in (d). This is due

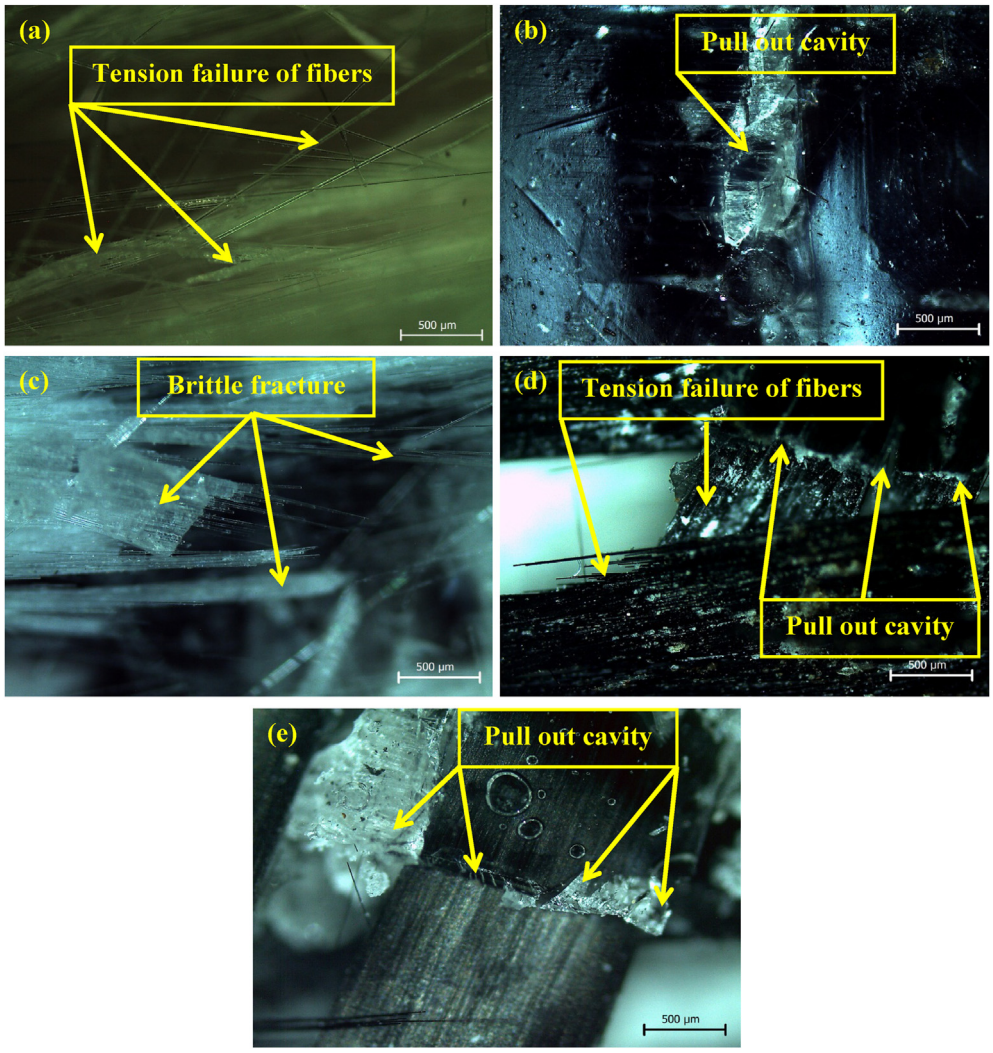

Fig. 10 – Fracture surfaces of prepared samples at: (a) S_1, (b) S_2, (c) S_3, (d) S_4, and (e) S_5.

to uniform scattering of the nanoparticles. The failure mode of pull out cavity was observed in the hybrid glass and carbon fibers at 3 wt. % Al_2O_3 in (e). This is due to some nanoparticles were agglomerated in some portions and in another portions were emptied. After presenting the whole results and discussions them in a detailed and clear manner, we can present conclusion and summary of this study in the next section.

4. Conclusion

This paper presents a successful method to synthesize glass, carbon, and hybrid FRPs with mixing nanocomposites by high-frequency sonication technique for wind turbine purposes. Different parameters have been investigated to obtain a new composite material with enhanced properties. The parameters include different nanoparticles' contents of Al_2O_3 and GNPs on woven glass fiber, carbon fiber and hybrid glass, and carbon fiber; concerning nanoparticles' dispersion through morphological, microstructural, and mechanical characteristics.

According to the reported observations from this study, the main conclusions can be summarized as follows:

1. The high-frequency sonication technique is found to be an efficient technique to disperse the different contents of nanoparticles (Al_2O_3 and GNPs) on woven hybrid glass and carbon fiber,
2. The highest hardness was obtained by hybrid glass and carbon fibers at weight fraction of 1.5% for both of GNPs and Al_2O_3 while the hybrid glass and carbon fiber obtained the ultimate tensile strength with weight fraction of 3% for Al_2O_3,
3. The microstructure refers to a perfect scattering and a better distribution of the GNPs and the Al_2O_3 in the hybrid glass and carbon fiber at weight fraction of 1.5% for both of GNPs and Al_2O_3,
4. The hardness values increase with increasing the dispersion of the GNPs and Al_2O_3 contents,
5. The mechanical properties fell with the absence of GNPs and Al_2O_3. This was due to the progressive influence on the grain growth mechanism and the agglomeration of GNPs and Al_2O_3,

6. The flexural strength of the Al_2O_3 reinforced nanocomposites with weight fraction of 3% attained its optimum value and gradually decreased after that for the high concentration of weight fraction of 1.5% of GNPs and weight fraction of 1.5% of Al_2O_3, and
7. The experimental results reveal that the best weight fraction of GNPs and Al_2O_3, is 1.5% which improves the microstructural characterization and mechanical properties of the hybrid glass and carbon fibers.

These conclusions can be attributed to the improvement of both the microstructural characterization and mechanical properties of the hybrid glass and carbon fibers with weight fraction of 1.5% for both of GNPs and Al_2O_3.

Declaration of Competing Interest

The authors declare that there is no conflict of interest.

Acknowledgment

This work was supported by the graduation projects program administered by the Office of National Research in the Academy of Scientific Research and Technology in Egypt under Grant No. 222. Also, the authors are highly grateful to the graduation project students at 2020–2021 in the Modern Academy for Engineering and Technology for useful their assistance in preparing some experimental work.

REFERENCES

[1] Willis D, Niezrecki C, Kuchma D, Hines E, Arwade S, Barthelmie R, et al. Wind energy research: state-of-the-art and future research directions. Renew Energy 2018;125:133–54.
[2] Walford CA. Wind turbine reliability: understanding and minimizing wind turbine operation and maintenance costs. Sandia National Laboratories; 2006.
[3] Kalkanis K, Psomopoulos CS, Kaminaris S, Ioannidis G, Pachos P. Wind turbine blade composite materials-end of life treatment methods. Energy Procedia 2019;157:1136–43.
[4] Ata MH, Abu-Okail M, Essa GM, Mahmoud T, Hassab–Allah I. Failure mode and failure load of adhesively bonded composite joints made by glass fiber-reinforced polymer. J Fail Anal Prev 2019;19:950–7.
[5] Abu-Okail M, Nafea M, Ghanem M, El-Sheikh M, El-Nikhaily A, Abu-Oqail A. Damage mechanism evaluation of polymer matrix composite reinforced with glass fiber via modified Arcan test specimens. J Fail Anal Prev 2020:1–11.
[6] Showaib EA, Elsheikh AH. Effect of surface preparation on the strength of vibration welded butt joint made from PBT composite. Polym Test 2020;83:106319.
[7] Elsheikh AH, Abd Elaziz M, Ramesh B, Egiza M, Al-qaness MAA. Modeling of drilling process of GFRP composite using a hybrid random vector functional link network/parasitism-predation algorithm. J Mater Res Technol 2021;14:298–311.
[8] AbuShanab WS, Elaziz MA, Ghandourah EI, Moustafa EB, Elsheikh AH. A new fine-tuned random vector functional link model using Hunger games search optimizer for modeling friction stir welding process of polymeric materials. J Mater Res Technol 2021;14:1482–93. https://doi.org/10.1016/j.jmrt.2021.07.031.
[9] Niezrecki C, Poozesh P, Aizawa K, Heilmann G. Wind turbine blade health monitoring using acoustic beamforming techniques. J Acoust Soc Am 2014;135:2392–3.
[10] Overgaard LCT, Lund E. Structural collapse of a wind turbine blade. Part B: progressive interlaminar failure models. Compos Part A Appl Sci Manuf 2010;41:271–83.
[11] Dass K, Chauhan S, Gaur B. Study on the effects of nano-aluminum-oxide particulates on mechanical and tribological characteristics of chopped carbon fiber reinforced epoxy composites. Proc IME Part L: J Mater Des Appl 2017;231:403–22.
[12] Khamaj A, Farouk WM, Shewakh WM, Abu-Oqail AMI, Wagih A, Abu-Okail M. Effect of lattice structure evolution on the thermal and mechanical properties of Cu–Al_2O_3/GNPs nanocomposites. Ceram Int 2021;47:16511–20.
[13] Kumar A, Lal S, Kumar S. Fabrication and characterization of A359/Al_2O_3 metal matrix composite using electromagnetic stir casting method. J Mater Res Technol 2013;2:250–4.
[14] Sharma VK, Kumar V. Development of rare-earth oxides based hybrid AMCs reinforced with SiC/Al_2O_3: mechanical & metallurgical characterization. J Mater Res Technol 2019;8:1971–81.
[15] Abu–Okail M, Shewakh W, Brisha AM, Abdelraouf YA, Abu-Oqail A. Effect of GNPs content at various compaction pressures and sintering temperatures on the mechanical and electrical properties of hybrid Cu/Al_2O_3/xGNPs nanocomposites synthesized by high energy ball milling. Ceram Int 2020;46:18037–45.
[16] Costa UO, Nascimento LFC, Garcia JM, Bezerra WBA, Fabio da Costa GF, Luz FSd, et al. Mechanical properties of composites with graphene oxide functionalization of either epoxy matrix or curaua fiber reinforcement. J Mater Res Technol 2020;9:13390–401.
[17] Garcia Filho FdC, Luz FSd, Oliveira MS, Pereira AC, Costa UO, Monteiro SN. Thermal behavior of graphene oxide-coated piassava fiber and their epoxy composites. J Mater Res Technol 2020;9:5343–51.
[18] Sardinha AF, Almeida DAL, Ferreira NG. Electrochemical impedance spectroscopy correlation among graphene oxide/carbon fibers (GO/CF) composites and GO structural parameters produced at different oxidation degrees. J Mater Res Technol 2020;9:10841–53.
[19] Li W, He D, Bai J. The influence of nano/micro hybrid structure on the mechanical and self-sensing properties of carbon nanotube-microparticle reinforced epoxy matrix composite. Compos Appl Sci Manuf 2013;54:28–36.
[20] Lephuthing SS, Okoro AM, Ige OO, Olunambi PA. Microstructural and electrochemical studies of spark plasma sintered multiwall carbon nanotubes reinforced TiO_2–MnO_2 based composite. J Mater Res Technol 2021;12:894–903.
[21] Elhousari AM, Rashad M, Elsheikh AH, Dewidar M. The effect of rubber powder additives on mechanical properties of polypropylene glass-fiber-reinforced composite. Mech Sci 2021;12:461–9.
[22] Krivoshapkin PV, Mishakov IV, Vedyagin AA, Bauman YI, Krivoshapkina EF. Synthesis and characterization of carbon/ceramic composite materials for environmental applications. Compos Commun 2017;6:17–9.
[23] Demiroglu S, Singaravelu V, Seydibeyoğlu MÖ, Misra M, Mohanty AK. 13-the use of nanotechnology for fibre-reinforced polymer composites. In: Seydibeyoğlu MÖ, Mohanty AK, Misra M, editors. Fiber technology for fiber-reinforced composites. Woodhead Publishing; 2017. p. 277–97.

[24] Abyzov A. Aluminum oxide and alumina ceramics (review). Part 1. Properties of Al_2O_3 and commercial production of dispersed Al_2O_3. Refract Ind Ceram 2019;60:24–32.
[25] Rivera T. Synthesis and thermoluminescent characterization of ceramics materials, Advances in ceramics-synthesis and characterization, processing and specific applications. INTECHOPEN; 2011.
[26] Abyzov A. Aluminum oxide and alumina ceramics (review). Part 2. Foreign manufacturers of alumina ceramics. Technologies and research in the field of alumina ceramics 1. Refract Ind Ceram 2019;60:33–42.
[27] Sun J, Gao L, Jin X. Reinforcement of alumina matrix with multi-walled carbon nanotubes. Ceram Int 2005;31:893–6.
[28] Puchy V, Hvizdos P, Dusza J, Kovac F, Inam F, Reece M. Wear resistance of Al2O3–CNT ceramic nanocomposites at room and high temperatures. Ceram Int 2013;39:5821–6.
[29] Yazdani B, Xia Y, Ahmad I, Zhu Y. Graphene and carbon nanotube (GNT)-reinforced alumina nanocomposites. J Eur Ceram Soc 2015;35:179–86.
[30] Porwal H, Grasso S, Reece M. Review of graphene–ceramic matrix composites. Adv Appl Ceram 2013;112:443–54.
[31] Chang Y, Bermejo R, Messing GL. Improved fracture behavior of alumina microstructural composites with highly textured compressive layers. J Am Ceram Soc 2014;97:3643–51.
[32] Devnani GL, Sinha S. Effect of nanofillers on the properties of natural fiber reinforced polymer composites. Mater Today: Proc 2019;18:647–54.
[33] Tian Y, Zhang H, Zhang Z. Influence of nanoparticles on the interfacial properties of fiber-reinforced-epoxy composites. Compos Appl Sci Manuf 2017;98:1–8.
[34] Talib AA, Abbud L, Ali A, Mustapha F. Ballistic impact performance of Kevlar-29 and Al_2O_3 powder/epoxy targets under high velocity impact. Mater Des 2012;35:12–9.
[35] Kaybal HB, Ulus H, Demir O, Şahin ÖS, Avcı A. Effects of alumina nanoparticles on dynamic impact responses of carbon fiber reinforced epoxy matrix nanocomposites. Eng Sci Technol Int J 2018;21:399–407.
[36] Mohanty A, Srivastava V. Effect of alumina nanoparticles on the enhancement of impact and flexural properties of the short glass/carbon fiber reinforced epoxy based composites. Fibers Polym 2015;16:188–95.
[37] Li W, Dichiara A, Zha J, Su Z, Bai J. On improvement of mechanical and thermo-mechanical properties of glass fabric/epoxy composites by incorporating CNT–Al_2O_3 hybrids. Compos Sci Technol 2014;103:36–43.
[38] Mudra E, Hrubovcakova M, Shepa I, Kovalcikova A, Girman V, Bures R, et al. Processing and characterization of fiber-reinforced and layered alumina-graphene composites. J Eur Ceram Soc 2020;40:4808–17.
[39] Güler Ö, Bağcı N. A short review on mechanical properties of graphene reinforced metal matrix composites. J Mater Res Technol 2020;9:6808–33.